Project Acronym:

MRBREASTBIO (CONCEPT/0521/0040)

MRI breast robotic system for biopsy

Deliverable number: 4.1

Title: Development of Agar/water phantom

Prepared by:

Anastasia Antoniou (CUT)
Christakis Damianou (CUT)

Date: 04/10/2022

Co-funded by the European Union

Republic of Cyprus

RESEARCH & INNOVATION FOUNDATION

Contents

Executive summary

The current deliverable concerns the development of a phantom model mimicking breast tissue and tumour to be utilized as the main tool for evaluating the developed biopsy robot in terms of Magnetic Resonance Imaging (MRI) compatibility and motion accuracy, as well as the functionality of the navigating software.

Agar was selected as the main ingredient of the phantoms for various reasons, such as the low cost and ease preparation of agar-based gels, as well as their ability to emulate critical properties of various body tissues, including the MR relaxation times T1 and T2.

MRI-guided biopsy phantoms should closely resemble the MRI properties of body tissues so as to offer realistic visualization and good contrast between embedded tumours and surrounding tissue in MRI. Therefore, different mixtures of agar and silicon dioxide powders were prepared and imaged in a 3T scanner for T1 and T2 mapping.

Phantom models containing one or multiple biopsy targets were then created. A phantom with tumour mimics of varying dimensions was also created to facilitate assessment of the needle targeting accuracy. The tumour mimics differed from the surrounding material in the concentration of inclusions. Aspects such as the phantom stiffness and contrast of the embedded tumour simulator in MRI images were considered to select the phantom materials and their concentration. Advantageously, a phantom containing a cherry tomato is also proposed as a cost-effective tool for assessing needle targeting simultaneously allowing visualization of the sampling procedure and direct confirmation of its success.

The developed phantoms were assessed in MRI. Generally, T1-weighted and T2-weighted Spin Echo imaging yielded phantom images of very good quality in terms of contrast and resolution depending on the concentration of inclusions. The slight difference in materials content between the tumour mimic and surrounding tissue resulted in excellent contrast between tumour and tissue. Furthermore, the proposed phantoms provided good haptic feedback during needle insertion.

Another experiment was conducted where the MR relaxation times of a pure agar gel containing a silica doped agar-based tumour mimic were measured at magnetic field strengths of 1.5 and 3 T. Both relaxation times of the silica-doped tumour mimic were lower than those estimated for the surrounding agar gel at both 1.5 T and 3 T since the addition of silica has been previously shown to have a negative effect on the relaxation times. T1 increased significantly as the field strength was increased from 1.5 to 3 T while T2 did not change very much, as expected.

Introduction

High quality breast biopsy phantoms constitute a valuable tool in needle biopsy training and experimentation, as well as in testing the needle positioning accuracy of robotic-assisted breast biopsy devices.

Commercially available breast biopsy phantoms are composed of patented realistic and durable breast tissue with several types of masses of varying sizes interspersed randomly throughout it. Membranes mimicking skin are utilized to cover the tissue proving realistic needle resistance to trainers [1][2][3][4]. In an effort to minimize needle-tracking artifacts, self-healing tissue-mimicking materials have been used by several companies [3][5][6].

The majority of marketed phantoms are designed for practice under US guidance. Blue Phantom (CAE Healthcare, Sarasota, USA) provides a training model suitable for US-guided Fine needle aspiration biopsy (FNAB), which contains 14 masses of varying echogenicity and sizes (4- to 11-mm) [5]. A similar product provided by another company (Kyoto Kagaku Co., Ltd, Kyoto, Japan) can be utilized for both FNA, Core needle (CN) and Vacuum-assisted (VA) sampling methods [1]. An opaque version of the phantom with colored targets imbedded in 3 levels is available, allowing visualization of the sampling procedure, as well as direct confirmation of its success. A Zerdine-hydrogel phantom that contains amorphous lesions; six green cystic masses (8-15 mm) and six black dense masses (6-12 mm) was designed by the Computerized Imaging Reference Systems (CIRS) company (CIRS, Inc., Norfolk VA, USA) [6]. Another US breast biopsy phantom available in the market (Sun Nuclear Corporation, FL, USA) incorporates both fluid filled cysts (12 to 15 mm) and solid masses (7 to 10 mm) [4].

A clear gel wrapped in soft vinyl to provide compression ability and skin-like resistance is provided by Sun Nuclear company for stereotactic-guided biopsy training [4]. Solid gel lesions sized between 2 to 5 mm and liquid dye lesions were implanted within to be utilized for CN and FNA biopsy practice, respectively. Another compressible stereotactic needle biopsy phantom was manufactured by CIRS, where a proprietary gel embeds seven dense masses in three different sizes and two microcalcification clusters [2].

A beneficial phantom manufactured by CIRS is compatible with both US, X-ray, and MRI guided biopsy procedures [3]. The triple-modality phantom contains dense Zerdine-based spherical lesions with 100-300 micron microcalcification implanted within them, dense spiculated shape lesions, as well as cystic lesions containing water with green dye, thus facilitating lesion identification.

Not only commercially available, but also “laboratory” phantoms have been proposed over time for biopsy training purposes. In fact, many institutions preferred “home-made” alternatives for their studies, utilizing food or animal products, since they are of lower-cost and easy to make. Turkey or chicken breast, as well as gel-based breast phantoms are commonly used to simulate soft tissue [7]. However, it seems that chicken and turkey breast are more realistic regarding mechanical properties [8]. The inserts could be of liquid or solid content depending on the type of biopsy procedure that will be followed.

For freehand US-guided breast biopsy training, raw materials including olives with pimentos, capers, grapes, peas, potatoes, and strawberries have been proposed in the literature to mimic breast masses [7]. For example, Ng et al. developed [7] a gelatin-based phantom intended to improving the skill level of trainees, where the cysts were simulated by rubber gloves filled with colored solution, the benign tumors by dried sweet potatoes and dried agar konjac, while the malignant ones by pickled shallots carved into an irregular shape.

The same approach was followed in other studies, in which household and raw materials were selected for mimicking lesions in MR-compatible breast phantoms. In one study [9], the reliability of an MR-guided biopsy procedure with the assistance of an active marker was tested in agarose phantoms containing 7-mm diameter peas. It should be noted that peas possess short T1 and thus are easily visible on the MR images [9]. In addition, their composition and soft consistence make them ideal for biopsies [9]. The success of all biopsies was confirmed by visual inspection of the specimen. Furthermore, an automated system designed for lesion localization while operating at the isocenter of an MRI scanner was evaluated in a grapefruit phantom, in which the artificial lesions were vitamin E capsules (12 x 7 mm in size) [10]. Accurate biopsies were confirmed by detecting the capsule material in the specimen chamber of the biopsy device. Breast tissue was also mimicked by a grapefruit in the framework of another study [11]. Specifically, a long wooden dowel of 1 mm diameter was embedded into a grapefruit to form the final phantom. CN biopsy trials were performed using an MR-guided breast lesion localization and core biopsy system. The success of the procedure was defined by whether pieces of the wooden dowel were contained within the sample, as well as from the void showed up on follow up MRI [11].

The feasibility of US-guided biopsy systems to target artificial lesions with high accuracy was assessed in Poly(vinyl alcohol) cryogel (PVA-C) and chicken phantoms [12], [8]. The biopsy success was assessed by targeting the lesions which were simulated by hyperechoic, colored PVA-C, interspersed in the PVA-C phantoms [12], [8], as well as by hypo-echoic, clear PVA-C imbedded in the chicken tissue [12]. Except from PVA-C, mixtures of agar were utilized to mimic the breast tissue. Agar blocks with stainless steel beads were used for validation of needle placement accuracy of US-guided biopsy systems [12], [13]. In terms of MR-guided biopsy procedures, PVA-C was also utilized to imitate the breast tissue in several studies [14], [15]-[16]. In one study, phantoms were manufactured by pouring hot mixture of PVC into a 3D printed breast shaped mold [16]. Lesions, with a size varying from 5 to 20 mm, were simulated by fish oil capsules or pieces of stiff PVC added in the phantoms during the cool-off procedure. Note that PVA-C was widely used as a tissue mimic due to its robust mechanical properties [12]. Moreover, PVA-C has similar acoustic properties, as well as similar T1 and T2 relaxation times as human tissue, thus offering realistic visualization on both MRI and US [14].

Gadopentetate dimeglumine (Gd-DTPA), which is a commonly used contrast agent for MR imaging [17], can be added in gel-based lesion mimics to improve the MRI contrast with respect to the surrounding breast-mimicking tissue. In [18], authors attempted to determine the accuracy of an MR-guided 14-gauge core-needle biopsy device in a lard breast phantom. Gelatin-based lesions (6–7 mm) containing Gd-DTPA and methylene blue dye were created at random positions in the tissue. Visualization of blue dye in specimens confirmed the success of the biopsy. An MR compatible device for wire lesion localization was proposed by authors in [19]. The accuracy test involved MR-guided localization of lesions in a commercially available breast phantom (CIRS), as well as in cadaveric breasts, in which the lesions were simulated by surgically placed balloons (5-10 mm) containing a 1/60 solution of gadolinium-water. In vivo experiments in porcine animal models were also performed for evaluating the performance of a vacuum-assisted breast biopsy device [17]. In this study the lesions were created by injecting the animals with an aqueous gel containing Gd-DTPA. In another study [20], a mixture of lard and egg whites simulated the tissue, while a static lesion was introduced by molding a gadolinium-doped water solution into the tissue.

Breast biopsy phantoms for multimodal imaging have also been manufactured in-house. A dual modality; MRI and US breast phantom was designed using 10% PVA-C and a glass bead or a fiducial marker to simulate the target [14]. Notably, specially designed markers visible under both US, MRI and mammography imaging were proposed by authors in [21]. Another study

proposes a gelatin based phantom designed for breast interventions under CT, US and MRI guidance [22]. During the cool-off time, a part of the phantom was extracted and the void was filled with a special solution containing BaSO4 powder for CT contrast and CuSO4 for MRI contrast [22]. Recently, a 3D printing method was used for the construction of a triple-modality (US, mammography, and MRI) phantom eliminating any sanitary concerns may accompany the use of food products [23]. The breast tissue was a mixture of PVC powder and softener. Inserts were 3D printed using Acrylonitrile butadiene styrene (ABS) material having imbedded holes of different dimensions to simulate cylindrical and hemispherical tumors. This was done to assess the imaging quality and detection sensitivity in terms of lesion size.

Either commercially available or "home-made" phantoms utilizing household raw and laboratory materials are of great use in providing learning experiences to the future clinicians as well as in testing the accuracy of robotic assisted breast biopsy devices and procedures.

T1 and T2 of agar-based phantoms

Methodology

Test phantoms preparation

Agar-based phantoms with different concentrations of inclusions were prepared and contained in the rectangular container shown in **Figure 1A**, along with two reference liquids (water, oil). Agarose (Merck KGaA, EMD Millipore Corporation, Darmstadt, Germany) and silicon dioxide (Sigma-Aldrich, St. Louis, Missouri, United States) were utilized in different concentrations to demonstrate their effect on MRI properties. Three phantoms were prepared with varying concentration of agarose of 2 – 6 % weight per volume (w/v), which serves as the gelling agent. Various amounts of silicon dioxide (2– 8 % w/v) were added in phantoms with a fixed concentration of 6 % w/v agar. A detailed description of the preparation process can be found in a study by Drakos et al [24].

Experimental setup & procedure

The container was sited on the table of a 3T MR scanner (MAGNETOM Vida, Siemens Healthineers, Erlangen, Germany) for imaging. The Biomatrix 12 channel body coil (Siemens Healthineers) was properly positioned at sufficient distance above the container using a supporting structure. The experimental setup can be seen in **Figure 1B**.

Figure 1: (A) Photo of the phantoms in the container and the corresponding recipe used for each one. (B) The experimental setup for T1 and T2 measurements.

<u>*Variable Flip Angle T1 Mapping*</u>: Images of the phantoms were obtained in coronal plane using a Gradient Echo (GRE) sequence at variable flip angle (FA) of 5 - 26º for T1 mapping. The data were fitted into the following equation 1 [25]:

$$M_z = M_{0z}\left(\frac{1-e^{-\frac{TR}{T1}}}{1-\cos a\, e^{-\frac{TR}{T1}}}\right)\sin a \qquad [1]$$

where M_z is the longitudinal magnetization, M_{0z} is the magnetization at thermal equilibrium, TR is the pulse sequence repetition time, and a is the excitation flip angle. Image acquisition was performed using the following parameters: TR = 15 ms, echo time (TE) = 1.95 ms, echo train length (ETL) = 1, pixel bandwidth (pBW) = 277 kHz, matrix size = 160 x 160, slice thickness = 5 mm, and number of excitations (NEX) = 1.

Variable Echo Time T2 Mapping: A T2-weighted (T2-w) Spin Echo (SE) sequence was employed for estimating the transverse relaxation time. Multiple scans were obtained at variable TE values of 13.8 - 69 ms and the measured signal intensity over TE was fitted to the exponential decay function of equation 2 [26]:

$$M_{xy} = M_{xy0} e^{-\frac{TE}{T_2}} \quad [2]$$

where M_{xy} is the transverse magnetization and M_{xy0} is its maximum value. The images were acquired with the following parameters: TR = 1910 ms, TE = 13.8 – 69 ms, FA = 180º, ETL = 5, pBW = 228 kHz, matrix size = 160 x 160, slice thickness = 3 mm, and NEX = 1

The MR relaxation times of each phantom were estimated through a voxel-by-voxel analysis, where parametric maps were derived from the series of acquired images by fitting the mathematic models to the acquired data for each individual voxel through automated algorithmic processing.

Results

The phantoms were initially scanned using a GRE sequence at FA values ranging from 5 - 26º. **Figure 2** shows indicative coronal images acquired at FA within this range. **Table 1** lists the mean value of T1 and corresponding standard deviation for each phantom as estimated by the voxel-by-voxel analysis.

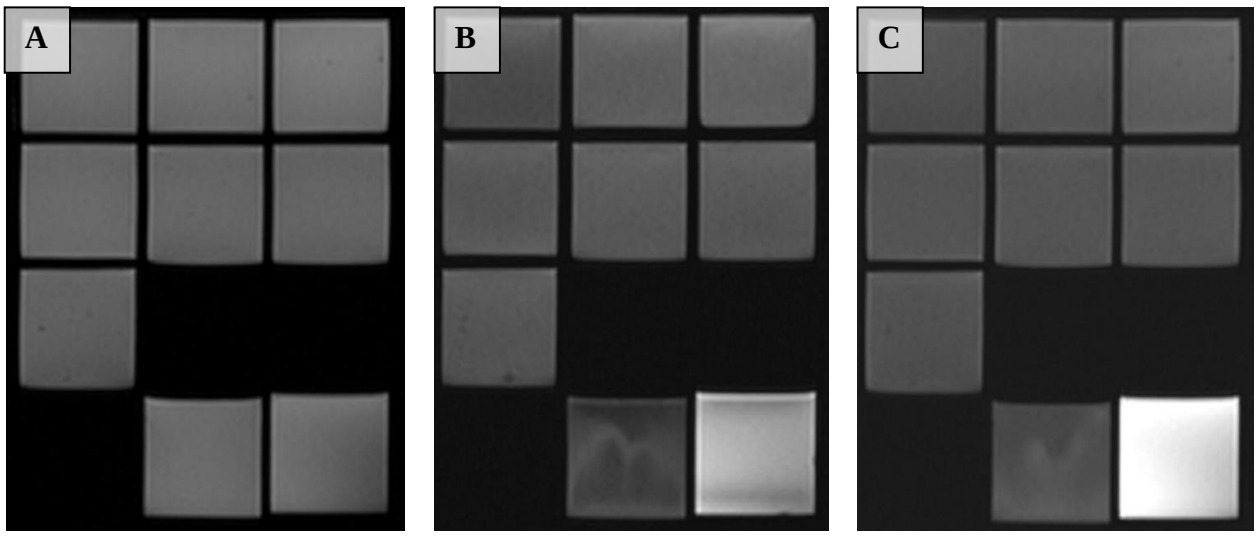

Figure 2: Coronal slices of the phantoms acquired using a GRE sequence at FA of (A) 5º (B) 21º (C) 26º. Imaging parameters: TR = 15 ms, TE = 1.95 ms, ETL = 1, pBW = 277 kHz, matrix size = 160 x 160, slice thickness = 5 mm, and NEX = 1 (SL = 99.6002).

Table 1: Mean T1 and standard deviation (SD) of phantoms as estimated by voxel-based analysis.

Phantom #	Material Composition	T1 (ms)	SD (ms)
1	2 % agar	3080.1	121
2	4 % agar	2486.2	53.9
3	6 % agar	2137.9	30.5
4	6 % agar, 2% silica	2259.6	41.2
5	6 % agar, 4% silica	2040.7	47
6	6 % agar, 6% silica	2039.2	38.4
7	6 % agar, 8% silica	1975	54.2
8	Water	3468.9	238.6
9	oil	309.8	4.3

Imaging of phantoms was then done using a T2-w SE sequence at various TE values in the range of 13.8 to 69 ms. Indicative images are presented in **Figure 3**. **Table 2** lists the mean value of T2 and the corresponding standard deviation for each phantom as estimated by the voxel-by-voxel analysis.

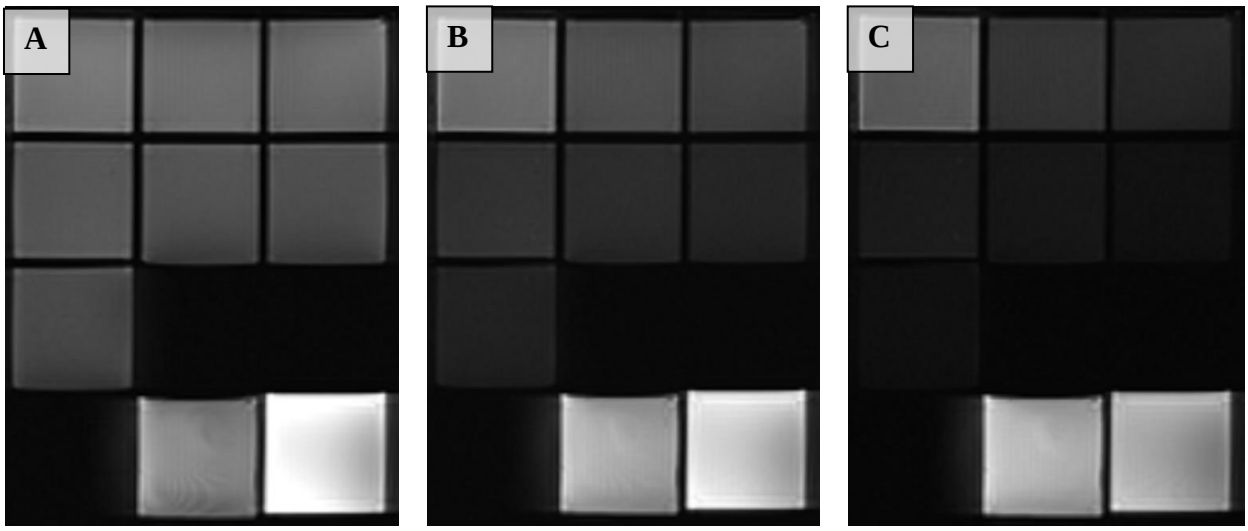

Figure 3: Coronal slices of the phantoms acquired using a T2-w SE sequence at TE values of (A) 13.8 (B) 41.4 (C) 69. Imaging parameters: TR = 1910 ms, FA = 180º, ETL = 5, pBW = 228 kHz, matrix size = 160 x 160, slice thickness = 3 mm, and NEX = 1 (SL = 108.455).

Table 2: Mean T2 and standard deviation (SD) of phantoms as estimated by voxel-based analysis.

Phantom #	Material Composition	T2 (ms)	SD (ms)
1	2 % agar	111.7	2.6
2	4 % agar	53.3	1.5
3	6 % agar	40.2	2.2
4	6 % agar, 2% silica	32.9	0.8
5	6 % agar, 4% silica	29.7	0.7
6	6 % agar, 6% silica	23.8	0.6
7	6 % agar, 8% silica	22.7	0.7
8	Water	96.4	2
9	oil	-	-

Typical phantoms

Phantom models containing one or multiple biopsy targets were then created. The selection of material concentration was mainly based on the T1 and T2 measurements of the various agar-silica mixtures, but also on other parameters, such as the phantom stiffness. In fact, the silica concentration of 8 % w/v (in a 6 % w/v agar gel) resulted in a very stiff phantom, whereas the agar concentration of 2 % w/v (pure agar gel) resulted in a slightly loose phantom. Therefore, the specific recipes were abandoned. Among the remaining recipes, different combinations of two mixtures (tumour and breast tissue) with notable difference in both T1 and T2 were made for phantom development. The different phantom models developed are presented below.

Single-tumour model

A phantom model containing a single large tumour mimic was developed, as shown in **Figure 4**. The breast tissue was mimicked by a 4% w/v agar gel. A spherical phantom of 6% w/v agar, 4% w/v silica, and 30% w/v milk was embedded in the agar gel to mimic a large tumour.

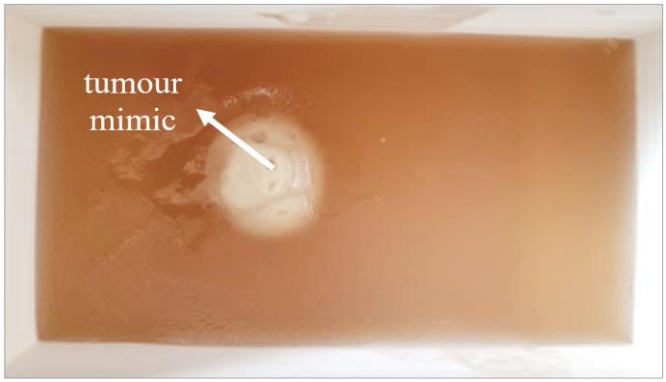

Figure 4: Photo of the single-tumour model.

Multiple-tumour model

A square phantom with six similar targets was created by molding in a specially designed 3D printed mold. An agar gel was prepared using 6 % w/v agar and 2 % w/v silica to mimic breast tissue, whereas another mixture of 6% w/v agar and higher silica concentration of 6 % w/v was prepared to mimic tumour tissue. **Figure 5** shows the top view of the phantom.

Figure 5: Agar-based phantom with six similar biopsy targets.

Furthermore, a phantom with 3 biopsy targets of different size was developed, as shown in **Figure 6**. The tumour mimics were made out of water, agar (6 % w/v) and silica (4 % w/v), whereas in the surrounding tissue no silica was used (4 % w/v agar). The tumour mimics have a spherical shape and diameters of 5, 10, and 15 mm as shown in Figure 6.

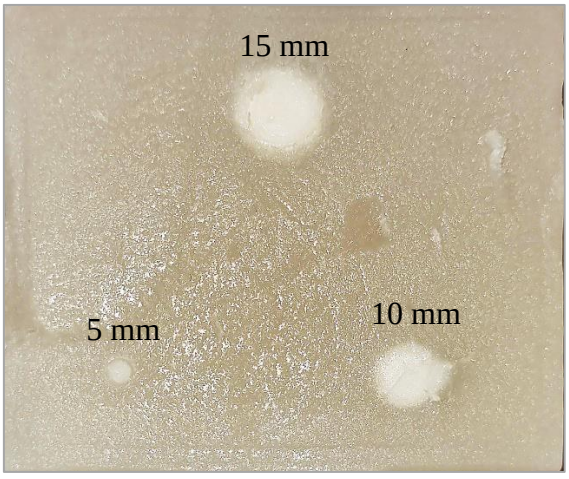

Figure 6: Agar-based phantom with biopsy targets of varying size (cross section).

Tumour model with cherry tomato

Finally, another tissue-tumour phantom was prepared by embedding a cherry tomato in pure agar gel of 4 % w/v. **Figure 7** is a photo of the phantom.

Figure 7: Photo of the agar phantom containing a cherry tomato.

MRI images of the phantoms

The large tumour phantom model was scanned in a 1.5T MRI scanner (GE Signa HD16, General Electric (GE), Chicago, Illinois, USA) using a body coil (HD BodyUpper, GE Healthcare Coils, Aurora, Ohio, USA). An indicative Spoiled gradient recalled echo (SPGR) image of the phantom is shown in **Figure 8**.

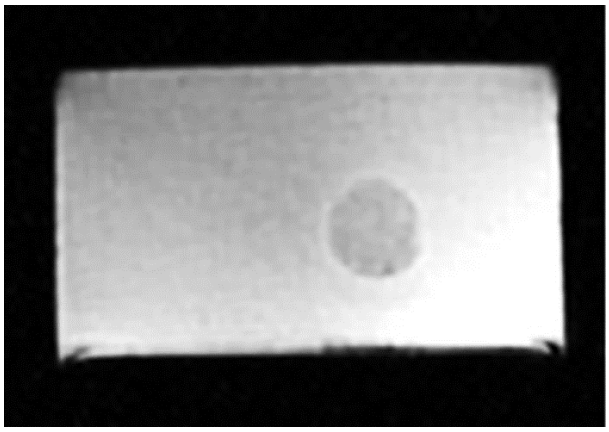

Figure 8: SPGR image of the phantom. Imaging parameters: TR = 20 ms, TE= 10ms, FA = 35°, ETL =1, PB = 28.75 Hz/pixel, FOV = 260 x 260 x 10 mm^3, NEX = 1, acquisition time/slice = 2.7 s.

Figures 9-11 present MRI images of the phantom containing six similar tumours, which were acquired in the 3T MR scanner (MAGNETOM Vida) using a multichannel body coil (18-channel, Siemens Healthineers). Similarly, **Figure 12** and **Figure 13** show MRI images of the phantom containing three spherical tumour mimics of varying diameter and the one containing a cherry tomato, respectively (at 3T).

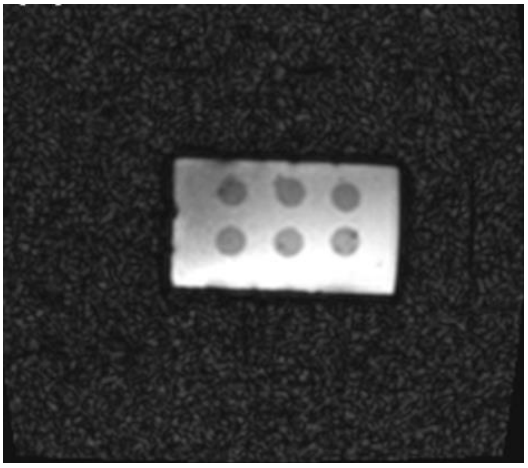

Figure 9: FLASH coronal image of the phantom containing 6 identical tumour mimics. Imaging parameters: TR = 25 ms, TE = 10 ms, FA = 30°, ETL = 1, NEX = 2, Pixel bandwidth = 240 Hz/pixel, FOV = 280 x 280 x 8 mm^3, matrix size = 128 x 128, slice thickness = 8 mm, and acquisition time/ slice = 3.2 mins.

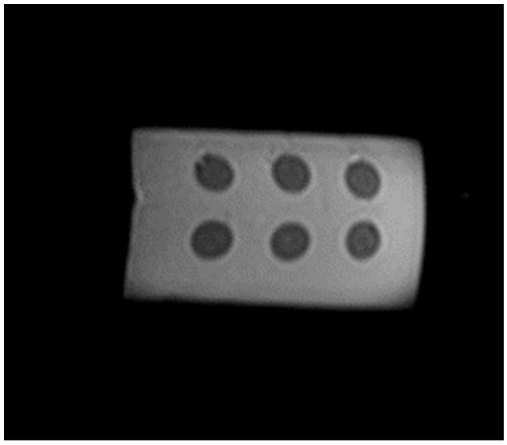

Figure 10: T1-w Turbo Spin Echo (TSE) coronal image of the phantom containing 6 identical tumour mimics. Imaging parameters: TR = 700 ms, TE = 23 ms, FA = 30°, ETL = 6, NEX = 2, Pixel bandwidth = 50 Hz/pixel, FOV = 280 x 280 x 10 mm^3, matrix size = 128 x 120, slice thickness = 10 mm, and acquisition time/ slice = 1 min.

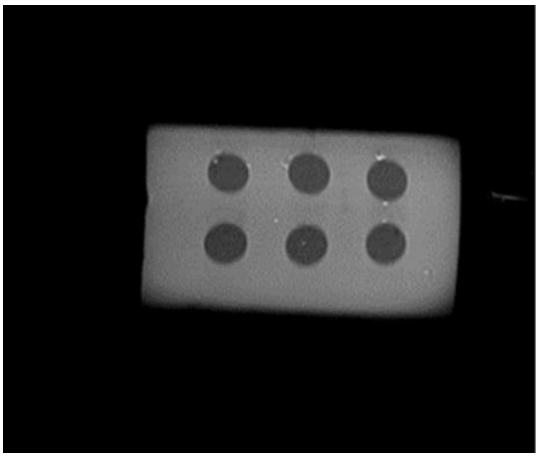

Figure 11: T2-w TSE coronal image of the phantom containing 6 identical tumour mimics. Imaging parameters: TR = 2500 ms, TE = 48 ms, FA = 180°, ETL = 16, NEX = 1, Pixel bandwidth = 50 Hz/pixel, FOV = 200 x 200 x 10 mm^3, matrix size = 320 x 320, slice thickness = 10 mm, and acquisition time/ slice = 2-3 mins

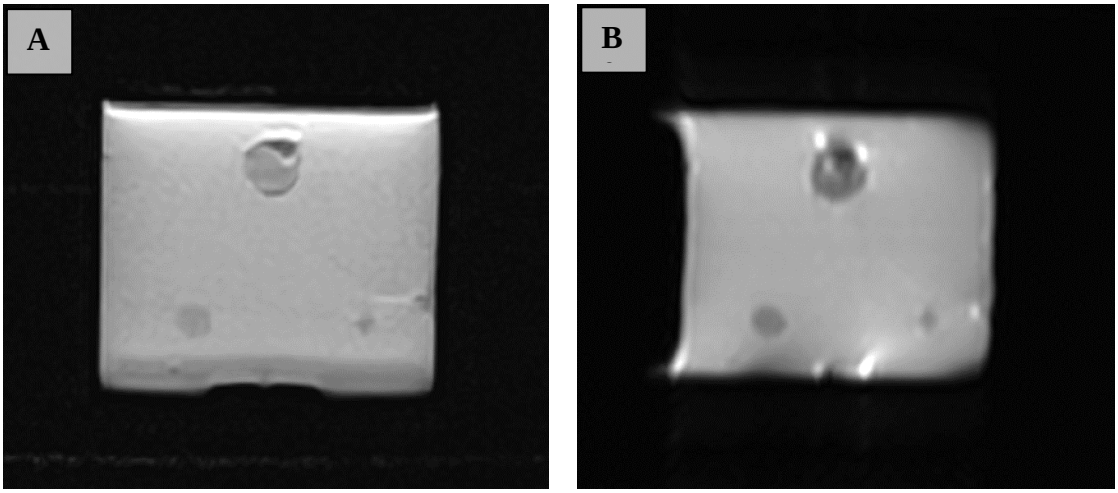

Figure 12: TSE coronal images of the phantom containing 3 tumour mimics of different size: (A) T1-w image with TR = 700 ms, TE = 22 ms, FA = 180°, ETL = 3, NEX = 2, Pixel bandwidth = 171 Hz/pixel, FOV = 200 x 200 x 8 mm^3, matrix size = 128 x 128, and slice thickness = 8 mm. (B) T2-w image with TR = 2500 ms, TE = 46 ms, FA = 180°, ETL = 8, NEX = 1, Pixel bandwidth = 50 Hz/pixel, FOV = 200 x 200 x 8 mm^3, matrix size = 128 x 128, and slice thickness = 8 mm.

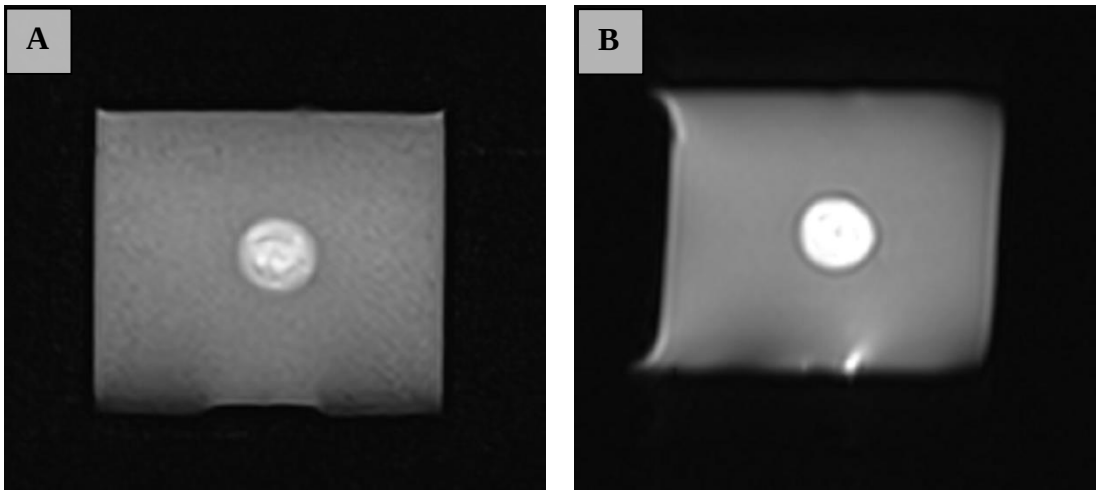

Figure 13: TSE coronal images of the phantom containing a cherry tomato: (A) T1-w image with TR = 700 ms, TE = 22 ms, FA = 180°, ETL = 3, NEX = 2, Pixel bandwidth = 171 Hz/pixel, FOV = 200 x 200 x 8 mm^3, matrix size = 128 x 128, and slice thickness = 8 mm. (B) T2-w image with TR = 2500 ms, TE = 46 ms, FA = 180°, ETL = 8, NEX = 1, Pixel bandwidth = 50 Hz/pixel, FOV = 200 x 200 x 8 mm^3, matrix size = 128 x 128, and slice thickness = 8 mm.

Measurement of T1 and T2 of single-tumour phantom at 1.5 and 3 T

Methodology

The T1 and T2 relaxation times of a single-tumour phantom were measured in the 3 T MRI scanner (Magnetom Vida), as well as in a 1.5 T MRI scanner (Signa HD16, GE Healthcare, Milwaukee, Wisconsin, USA). The phantom consisted of a pure agar gel of 6 % w/v concentration and an embedded tumour mimic of 6 % w/v agar and 4 % w/v silica. **Figure 14** shows the experimental setup for image acquisition, where the phantom was positioned on the table of the scanner with the coil placed at sufficient distance above its top surface with the assistance of a dedicated supporting structure.

Figure 14: Photo of the single-tumour phantom placed inside the 3 T MRI scanner with the imaging coil placed on top for MR image acquisition.

For image acquisition in the 3T scanner, an 18-channel body coil (Siemens Healthineers) was utilized, whereas in the 1.5 T scanner, the posterior head and face part of a head/neck/spine (HNS) coil (Signa 1.5T, 16 channel, GE Healthcare) was utilized.

A series of MR images were acquired for T1 & T2 mapping and inserted in a DICOM software (MicroDicom, MicroDicom Ltd., Sofia, Bulgaria) for post-processing. DICOM software tools were utilized for measuring the signal intensity (SI) in the phantom using a Region of Interest (ROI) approach. The mean SI was measured for ROIs in both the tumour mimic and agar-background.

Variable Inversion time T1 Mapping

For T1 relaxation time measurements, images of the phantom were acquired using a T1-w Inversion Recovery (IR) SE sequence at variable TI. The IR sequence is the standard method for T1 relaxation time measurements because of its large dynamic range and insensitivity to pulse sequence parameter imperfection. The mean SI measured in the selected ROI was plotted as a function of the varied TI used for image acquisition. The nulling TI (SI is zero) was interpolated from the graphs and the T1 relaxation time was calculated using Equation 1:

$$TI = 0.693 \times T1 \quad [3]$$

T1 relaxation measurements inside the 3 T MRI scanner (Magnetom Vida, Siemens Healthineers) were additionally performed using a voxel-by-voxel approach. In this regard, parametric maps were generated from the acquired MRI images using automated algorithms integrated in the MRI scanner.

For measurements in the 1.5 T MRI scanner with the IR sequence the following parameters were used: TR=5000 ms, TE=10.3 ms, FOV=260×260 mm^2, slice thickness=7 mm, matrix=192×128, NEX=0.5, ETL=15, FA=90^o, and TI values ranging from 50-1050 ms. Concerning measurements in the 3 T MRI scanner, the following parameters were utilized: TR=6320 ms, TE=9 ms, FOV=200×200 mm^2, slice thickness=10 mm, matrix=128×96, NEX=1, ETL=3, FA=180^o and TI values ranging from 150-3000 ms.

Variable Echo time T2 Mapping

For T2 relaxation time measurements, images of the agar-based phantoms were acquired using a T2-w SE sequence at variable TE. The mean SI measured in the selected ROI was plotted as a function of the varied TE and fitted to equation [2]. Specifically, following regression analysis, an exponential trendline was fitted to the plotted data and T2 relaxation time calculations were performed by taking the inverse of the exponent of the exponential fit.

The phantom was scanned inside the 1.5 T MRI scanner using a T2-W SE sequence with the following parameters: TR=2500 ms, FOV=260×260 mm^2, slice thickness=7 mm, matrix=192×128, NEX=2, ETL=14, FA=90^o and TE values ranging from 52.2-243.5 ms. For measurements inside the 3 T MRI scanner, the following parameters were utilized: TR=250 ms, FOV=260×260 mm^2, slice thickness=10 mm, matrix=128×128, NEX=2, ETL=12, FA=180^o and TE values ranging from 8.6-69 ms.

Results

Figure 15 shows a typical MRI image of the phantom acquired with the IR sequence inside the 3 T scanner (Magnetom Vida, Siemens Healthineers). **Figure 16** shows the plots of the mean SI measured within the ROIs in the tumour mimic (6 % w/v agar, 4 % w/v silica) and the agar-based background (6 % w/v agar) as a function of the varied TI (150-3000 ms), showcasing T1 magnetization recovery at 3T.

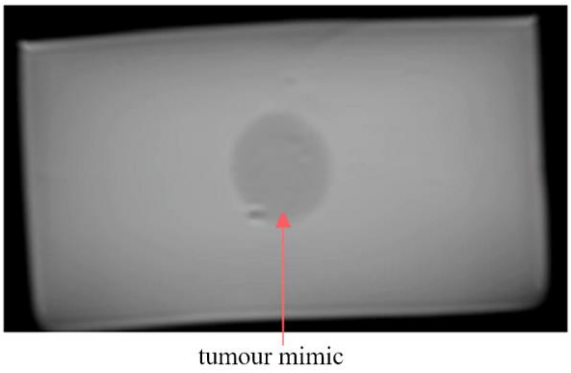

Figure 15: Coronal IR image of the single-tumour phantom acquired using a TI of 400 ms at 3T.

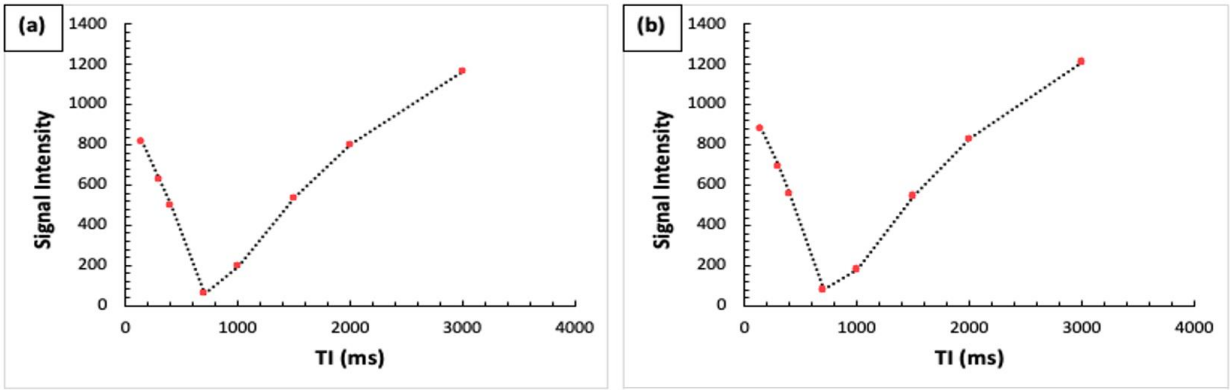

Figure 16: Signal intensities as measured from images acquired with an IR sequence inside a 3 T MRI scanner using varied TI values (150-3000 ms) for the (a) tumour mimic (6 % w/v agar, 4 % w/v silica), and (b) agar-based phantom (6 % w/v agar).

Accordingly, **Figure 17** shows a typical MRI image of the phantom acquired with the T2-w SE sequence inside the 3 T scanner (Magnetom Vida, Siemens Healthineers). **Figure 18** shows plots of the mean SI measured within the selected ROIs in the tumour mimic (6 % w/v agar, 4 % w/v silica) and the agar-based background (6 % w/v agar) as a function of the varied TE (13.8-138 ms), showcasing T2 magnetization decay at 3T.

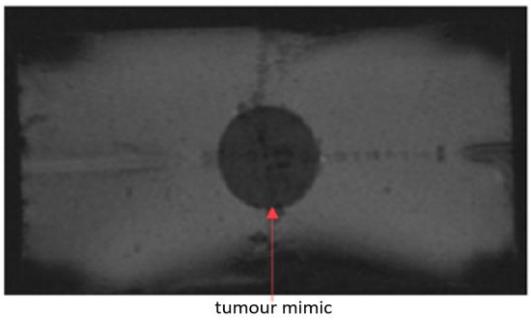

Figure 17: Coronal T2-w SE image of the phantom acquired using a TE of 34.52 ms at 3 T.

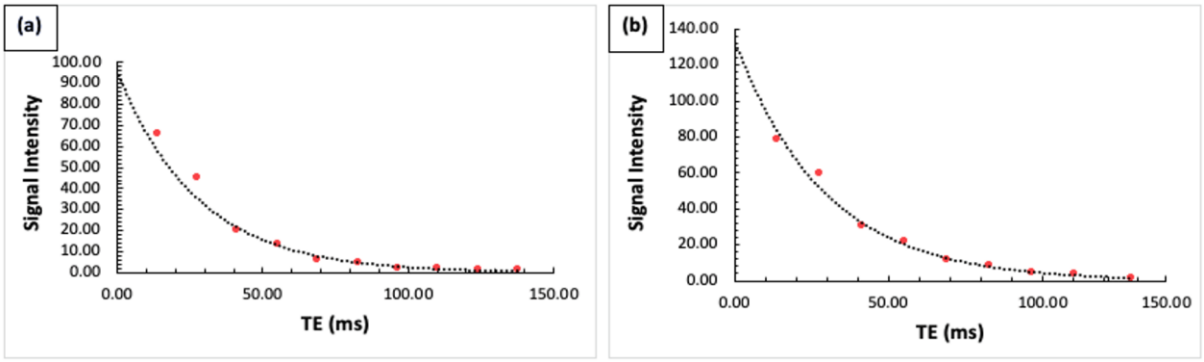

Figure 18: Signal intensities as measured from images acquired with a T2-W SE sequence inside a 3 T MRI scanner using varied TE values (13.8-138 ms) for the (a) tumour mimic (6 % w/v agar, 4 % w/v silica) and (b) agar-based phantom (6 % w/v agar).

Table 3 lists the T1 relaxation times as measured using IR sequences by the ROI approach inside a 1.5 T MRI scanner (Signa HD16, GE Healthcare), as well by a parametric map using voxel-by-voxel approach inside a 3 T MRI scanner (Magnetom Vida, Siemens Healthineers) for both the tumour mimic and surrounding agar gel. The T2 relaxation times as measured inside both MRI scanners using the ROI approach are also listed.

Table 3: Estimated T1 and T2 relaxation times of the agar gel and tumour mimic at 1.5 T and 3 T.

Material	**T1 (ms)**		**T2 (ms)**	
	1.5 T (ROI approach)	**3 T (Voxel approach)**	**1.5 T (ROI approach)**	**3 T (ROI approach)**
Tumour mimic (6 % agar & 4 % silica)	976.4	2099.2	43.7	45.71
Agar-phantom (6 % w/v agar)	1051.46	2135.76	45	40

Discussion

Tissues are characterized by two relaxation times; T1 and T2 that describe the rate at which protons return to equilibrium after a radiofrequency pulse. The contrast in MR images emerges from changes in the relaxation times and proton density of tissues, depending on the specific imaging sequence employed [27]. Accordingly, phantoms intended for MRI-guided breast biopsy should closely resemble the relaxation properties of body tissues so as to offer realistic visualization and good contrast between embedded tumours and surrounding tissue in MRI.

Therefore, T1 and T2 measurements of different agar-based mixtures were initially conducted. The effect of varying the agar and silica concentration on the relaxation times was investigated. Both T1 and T2 were gradually decreased with increasing agar concentration (2-6 % w/v). The same behavior was observed with increasing silica concentration (2-8 % w/v). Note that oil T2 relaxation could not be measured because of chemical shift artifacts that were obscuring the location of the measurement. The estimated T2 relaxation times ranged from 23 to 112 ms (3T) and are partly consistent with the values reported for soft tissues in a review article by Bottomley et al. [28] roughly ranging from 40 to 80 ms. Regarding the longitudinal relaxation time T1, literature values (at 3 T) are harshly between 500 – 1000 ms [29] for soft tissues and 898 to 1509 ms for muscle [26]. The T1 estimates (3T) for the agar-based phantoms are higher, ranging from 1975 to 3080 ms.

Several phantoms containing one or multiple biopsy targets of similar or different size were created. Agar-based mixtures with notable difference in both T1 and T2 were selected to mimic tumour and breast tissue so as to achieve proper delineation of the biopsy target in MRI. Note that the silica concentration of 8 % w/v (in a 6 % w/v agar gel) and agar concentration of 2 % w/v (pure agar gel) were abandoned since they resulted in a very stiff and slightly loose phantoms, respectively. A pure agar gel containing a cherry tomato has also been proposed.

Imaging of the various phantom models was performed using different MRI sequences. Generally, the T1-w and T2-w SE imaging yielded phantom images of very good quality. To be more specific, for the phantom (6% w/v agar, 2% silica) containing 6 identical tumour mimics (6% w/v agar, 6% silica), T2-w SE imaging provided the best quality in terms of contrast and resolution (for the specific imaging parameters employed) whereas for the phantom (4% w/v agar) containing three tumour mimics (6% w/v agar, 4% silica) of varying size and the one with the cherry tomato, the T1-w imaging resulted in clearer images with better delineation of phantom and tumour edges.

Finally, another experiment was conducted where the MR relaxation times of a pure agar gel (6 % w/v agar) containing a silica doped tumour mimic (6 % w/v agar, 4 % w/v silica) were measured at magnetic field strengths of 1.5 and 3 T. A series of T1-w IR images at varying TI and a series of T2-w images at varying TE were acquired for T1 and T2 mapping, respectively, where the mean SI values measured in specific ROIs were fitted to the mathematical models of transverse and longitudinal magnetizations. T1 mapping in the 3 T scanner was also done using a voxel-by-voxel approach by generating parametric maps.

The T1 and T2 relaxation times of the agar-phantom were higher than those estimated for the tumor-like material at both 1.5 T and 3 T, since the addition of silica has been previously shown to have a negative effect on the relaxation times [30]. T1 increased significantly as the field strength was increased from 1.5 to 3 T while T2 did not change very much, as expected.

Overall, the slight difference in materials content between the tumour mimics and surrounding materials resulted in excellent contrast between tumour and tissue in MRI. This is an excellent breast tissue/tumour model that can be used to evaluate the functionality of MRI-guided biopsy devices and may also be used for training purposes.

References

[1] "Ultrasound-Guided Breast Biopsy Phantom | Products: Patient Simulators for Diagnostic Training | Kyotokagaku Co., Ltd.," *Kyotokagaku.com*. [Online]. Available: https://www.kyotokagaku.com/products/detail01/us-9.html. [Accessed: 14-Jul-2020].

[2] "Stereotactic Needle Biopsy Phantom - CIRS," *CIRS*. [Online]. Available: https://www.cirsinc.com/products/mammography/stereotactic-needle-biopsy-phantom/. [Accessed: 14-Jul-2020].

[3] "Multi-Modality Breast Biopsy and Sonographic Trainer - CIRS," *CIRS*. [Online]. Available: https://www.cirsinc.com/products/ultrasound/zerdine-hydrogel/multi-modality-breast-biopsy-and-sonographic-trainer/. [Accessed: 14-Jul-2020].

[4] "Sun Nuclear Breast Biopsy Phantoms (Gammex™ Technology) - Sun Nuclear," *Sunnuclear.com*. [Online]. Available: https://www.sunnuclear.com/products/breast-biopsy-phantom-s. [Accessed: 14-Jul-2020].

[5] "Blue Phantom breast ultrasound surgical training model," *Bluephantom.com*. [Online]. Available: https://www.bluephantom.com/product/Breast-Biopsy-Ultrasound-Training-Model.aspx?cid=438. [Accessed: 14-Jul-2020].

[6] "Ultrasound Needle Breast Biopsy Phantom with Amorphous Lesions - CIRS," *CIRS*. [Online]. Available: https://www.cirsinc.com/products/ultrasound/zerdine-hydrogel/ultrasound-needle-breast-biopsy-phantom-with-amorphous-lesions/. [Accessed: 14-Jul-2020].

[7] S. Y. Ng and C. Lin, "Low-cost and easily fabricated ultrasound-guided breast phantom for breast biopsy training," *Prepr. (Version 1) available Res. Sq.*, pp. 1–22, 2020, doi: 10.21203/rs.2.19957/v1.

[8] A. Fenster, K. J. M. Surry, G. R. Mills, and D. B. Downney, "3D ultrasound guided breast biopsy system," *Ultrasonics*, vol. 42, pp. 769–774, 2004, doi: 10.1016/j.ultras.2003.11.004.

[9] R. Werner *et al.*, "MR-Guided Breast Biopsy Using an Active Marker : A Phantom Study," *J. Magn. Reson. Imaging*, vol. 24, pp. 235–241, 2006, doi: 10.1002/jmri.20600.

[10] S. O. R. Pfleiderer, C. Marx, J. Vagner, R.-P. Franke, J. R. Reichenbach, and W. A. Kaiser, "Magnetic Resonance-Guided Large-Core Breast Biopsy Inside a 1.5-T Magnetic Resonance Scanner Using an Automatic System: In vitro Experiments and Preliminary Clinical Experience in Four Patients," *Invest. Radiol.*, vol. 40, no. 7, pp. 458–463, 2005, doi: 10.1097/01.rli.0000167423.27180.54.

[11] E. Schneider, K. W. Rohling, M. D. Schnall, R. O. Giaquinto, E. A. Morris, and D. Ballon, "An Apparatus for MR-Guided Breast Lesion Localization and Core Biopsy : Design and Preliminary Results," *J. Magn. Reson. Imaging*, vol. 14, pp. 243–253, 2001, doi: 10.1002/jmri.1180.

[12] K. J. M. Surry, W. L. Smith, L. J. Campbell, G. R. Mills, D. B. Downey, and A. Fenster, "The development and evaluation of a three-dimensional ultrasound-guided breast biopsy apparatus," *Med. Image Anal.*, vol. 6, pp. 301–312, 2002.

[13] W. L. Smith, K. J. M. Surry, G. R. Mills, D. B. Downey, and A. Fenster, "Three-Dimensional Ultrasound-Guided Core Needle Breast Biopsy," *Ultrasound Med. Biol.*, vol. 27, no. 8, pp. 1025–1034, 2001.

[14] A. M. Tang *et al.*, “Simultaneous Ultrasound and MRI System for Breast Biopsy : Compatibility Assessment and Demonstration in a Dual Modality Phantom,” *IEEE Trans. Med. Imaging*, vol. 27, no. 2, pp. 247–254, 2008, doi: 10.1109/TMI.2007.911000.

[15] W. Liu, Z. Yang, D. Feng, and D. Zhang, “Design and implementation of a new cable-driven robot for MRI-guided breast biopsy,” *Int. J. Med. Robot. Comput. Assist. Surg.*, vol. 16, no. 2, 2020, doi: 10.1002/rcs.2063.

[16] V. Groenhuis, F. J. Siepel, J. Veltman, J. K. van Zandwijk, and S. Stramigioli, “Stormram 4: An MR Safe Robotic System for Breast Biopsy,” *Ann. Biomed. Eng.*, vol. 46, no. 10, pp. 1686–1696, 2018, doi: 10.1007/s10439-018-2051-5.

[17] B. L. Daniel *et al.*, “An MRI-Compatible Semiautomated VacuumAssisted Breast Biopsy System: Initial Feasibility Study,” *J. Magn. Reson. Imaging*, vol. 644, pp. 637–644, 2005, doi: 10.1002/jmri.20302.

[18] B. L. Daniel, R. L. Birdwell, J. W. Black, D. M. Ikeda, G. H. Glover, and R. J. Herfkens, “Interactive MR-guided, 14-gauge core-needle biopsy of enhancing lesions in a breast phantom model,” *Acad. Radiol.*, vol. 4, no. 7, pp. 508–512, 1997, doi: 10.1016/S1076-6332(97)80238-3.

[19] D. P. Gorczyca, D. Debruhl, and C. Sullenberger, “Wire Localization of Breast Lesions Before Biopsy : Use of an MR-Compatible Device in Phantoms and Cadavers,” *Am. J. Roentgenol.*, vol. 165, pp. 835–838, 1995, doi: 0.2214/ajr.165.4.7676977.

[20] M. Freed, R. H. El Khouli, K. J. Myers, M. H. Greene, J. H. Duyn, and A. Badano, “An anthropomorphic phantom for quantitative evaluation of breast MRI,” *Med. Phys.*, vol. 38, no. 2, pp. 743–753, 2011, doi: 10.1118/1.3533899.

[21] J. A. Kaplan, M. W. Grinstaff, and B. N. Bloch, “Polymer film-nanoparticle composites as new multimodality, non-migrating breast biopsy markers,” *Eur. Radiol.*, vol. 26, no. 3, pp. 866–873, 2016, doi: 10.1007/s00330-015-3852-7.

[22] M. Ruschin, S. R. H. Davidson, W. Phounsy, L. Chin, A. Ravi, and C. Mccann, “Technical Note : Multipurpose CT, ultrasound, and MRI breast phantom for use in radiotherapy and minimally invasive interventions,” *Med. Phys.*, vol. 43, no. 5, pp. 2508–2514, 2016, doi: 10.1118/1.4947124.

[23] Y. He *et al.*, “3D-printed breast phantom for multi-purpose and multi-modality imaging,” *Quant. Imaging Med. Surg.*, vol. 9, no. 1, pp. 63–74, 2019, doi: 10.21037/qims.2019.01.05.

[24] T. Drakos, M. Giannakou, G. Menikou, G. Constantinides, and C. Damianou, “Characterization of a soft tissue-mimicking agar/wood powder material for MRgFUS applications,” *Ultrasonics*, vol. 113: 10635, 2021, doi: 10.1016/j.ultras.2021.106357.

[25] G. Liberman, Y. Louzoun, and D. Ben Bashat, “T1 Mapping using variable flip angle SPGR data with flip angle correction,” *J. Magn. Reson. Imaging*, vol. 40, no. 1, pp. 171–180, 2014, doi: 10.1002/jmri.24373.

[26] J. Z. Bojorquez, S. Bricq, C. Acquitter, F. Brunotte, P. M. Walker, and A. Lalande, “What are normal relaxation times of tissues at 3 T?,” *Magn. Reson. Imaging*, vol. 35, no. 2017, pp. 69–80, 2017, doi: 10.1016/j.mri.2016.08.021.

[27] V. Rieke and K. B. Pauly, “MR Thermometry,” *J Magn Reson Imaging*, vol. 27, no. 2, pp. 376–390, 2008, doi: 10.1002/jmri.21265.MR.

[28] P. A. Bottomley, T. H. Foster, R. E. Argersinger, and L. M. Pfeifer, “A review of normal tissue hydrogen NMR relaxation times and relaxation mechanisms from 1–100 MHz: Dependence on tissue type, NMR frequency, temperature, species, excision, and age,” *Int. J. Med. Phys. Res. Pract.*, vol. 11, no. 4, pp. 425–448, 1984, doi: 10.1118/1.595535.

[29] G. J. Stanisz *et al.*, “T1, T2 relaxation and magnetization transfer in tissue at 3T,” *Magn. Reson. Med.*, vol. 54, no. 3, pp. 507–512, 2005, doi: 10.1002/mrm.20605.

[30] A. Antoniou *et al.*, “MR relaxation times of agar-based tissue-mimicking phantoms,” *J. Appl. Clin. Med. Phys.*, p. 213533, 2022, doi: 10.1002/acm2.13533.